

# Pressure Leaching of Chalcopyrite Concentrate with Oxygen and Kinetic Study on the Process in Sulfuric Acid Solution

B. Mojtahedi<sup>1</sup> · S. Rasouli<sup>1</sup> · H. Yoozbashizadeh<sup>1</sup>

Received: 10 October 2019 / Accepted: 17 January 2020 / Published online: 6 March 2020  
© The Indian Institute of Metals - IIM 2020

**Abstract** In this research work, the pressure leaching of chalcopyrite concentrate with oxygen was studied. Experiments were carried out under conditions of the solid–liquid ratio of 0.1, agitation speed of 750 rpm, and sulfuric acid concentration of 2 M in a stainless-steel autoclave system under 0.6 to 1 MPa oxygen gas. Central composite design was used to design experiments, and three factors of temperature, time, and oxygen pressure were selected as the design variables. A linear model for %Cu and a quadratic model for %Fe were proposed by Minitab Software. The results showed that temperature is the most effective factor in chalcopyrite leaching. Under optimal conditions, 93.08% of copper with the aim of maximum dissolution was extracted. The kinetic study illustrated that the diffusion of the passive layer, produced during chalcopyrite leaching, controls the rate of the process. It can be represented by the  $1 - \frac{2}{3}\alpha - (1 - \alpha)^{\frac{2}{3}} = k_d t$  equation. The activation energy was calculated to be 14.19 kJ mol<sup>-1</sup>.

**Keywords** Pressure leaching · Chalcopyrite · Optimization · Kinetic study

## 1 Introduction

Copper in the earth's crust is most often found in the form of oxides, sulfides, carbonates, and native copper. But the most important sources of copper are copper sulfides, e.g., chalcopyrite (CuFeS<sub>2</sub>), bornite (Cu<sub>5</sub>FeS<sub>4</sub>), covellite (CuS), and chalcocite (Cu<sub>2</sub>S) [1]. One of the most abundant copper-bearing minerals is chalcopyrite (CuFeS<sub>2</sub>), which accounts for around 70% of the world's copper reservoir. Chalcopyrite concentrate is produced in a mineral concentration plant using various methods such as flotation [2]. Although more than 80% of copper is produced by pyrometallurgical methods, environmental pollution has led many researchers to focus on hydrometallurgical routes [3]. Using the hydrometallurgical process for copper extraction is not only environmentally friendly but also suitable for low-grade sulfide ores [4]. Extensive research has been carried out in the field of hydrometallurgy for the dissolution of copper from chalcopyrite in various media, and researchers have proposed different leaching media. These media are classified, according to the type of lixiviant to sulfate, chloride, ammonia, and nitrate [5–8]. Many studies about using different oxidizing reagents such as ferric and cupric ions, hydrogen peroxide, bacteria, and oxygen have been carried out in sulfuric acid solution under the atmospheric or pressure leaching conditions [9–13]. According to several research works, the initial reaction rate decreases over time. Researchers argued that the formed passive layer on mineral surfaces prevents the progress of dissolution. There are three different hypotheses to explain the nature of this produced layer. Its ingredients include elemental sulfur, polysulfide, or iron compound that have been known by various researchers [9]. Hackl et al. [14] believed that the passive layer on chalcopyrite particles is a copper-rich polysulfide, formed

✉ H. Yoozbashizadeh  
yoozbashi@sharif.edu

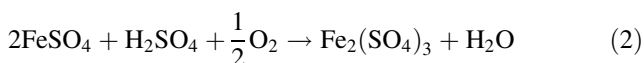
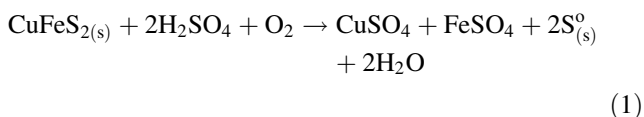
B. Mojtahedi  
behrad.mojtahedi25@student.sharif.ir

S. Rasouli  
Saleh.rasouli@gmail.com

<sup>1</sup> Department of Materials Science and Engineering (Extractive Metallurgy), Sharif University of Technology, Tehran, Iran

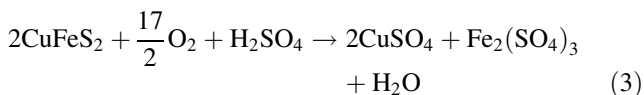
in initial steps and controls the leaching process. Temperature and acidity are two influential factors in the formation of sulfate and sulfur so that increasing temperature and decreasing acidity are favorable conditions for sulfate formation. Pressure leaching not only provides favorable conditions for sulfate formation (high temperature) but also increases the leaching kinetics. Besides, this method has the potentiality to commercialize. So in recent years, the use of pressure leaching has been investigated for the treatment of sulfide minerals, and today, it is used for the treatment of zinc concentrate and gold ore [13]. Hence, its application to chalcopyrite concentrate is of interest for this research work.

Various chemical reactions have been proposed for leaching of chalcopyrite in sulfate solution with dissolved oxygen as the oxidant. Hiroyoshi [15] and Holliday [16] have suggested the following reactions for the leaching of chalcopyrite:

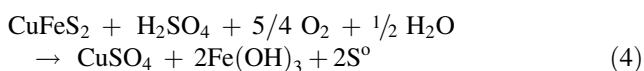


Yu et al. [17] studied the rate of chalcopyrite leaching in the sulfuric acid solution at the temperature range of 125–175 °C and the oxygen pressure range of 0.52 to 2.76 MPa.

They have noticed that slightly elemental sulfur is produced under these conditions and proposed the following reaction as the main reaction:



Vizsolyi et al. [18] dissolved chalcopyrite in a dilute sulfuric acid under conditions of 110° C and 3.4 MPa. They found that the elemental sulfur and hydrolyzed iron are produced during the leaching steps, and the major reaction is approximately as follows:



Pressure-oxidative leaching process, based on temperature, can be classified to low (< 100 °C), medium (140–180 °C), and high-temperature (> 200 °C)[19]. Depending on the purpose, chalcopyrite requires the effective parameters to be at their optimal level. Response surface methodology (RSM) is a set of mathematical and statistical techniques for constructing an empirical model in which several variables influence a response, and the aim is to optimize this response. One of

the advantages of RSM is the smaller number of empirical tests to analyze multiple parameters and their interactions [20, 21]. This study consists of modeling and optimizing the effective factors of copper and iron dissolution as a response. Then, the kinetics of the leaching process and activation energy are determined. Table 1 shows the activation energy in different leaching mediums and temperature ranges.

## 2 Thermodynamics of Chalcopyrite Dissolution

Pourbaix diagrams are used to identify predominant species in equilibrium with respect to the oxidation potential and pH of the solution. However, Eh–pH diagrams show only the equilibrium and do not provide information about reaction kinetics [30]. Figure 1 shows the Pourbaix diagram of the Cu–Fe–S system which is plotted by the HSC software at the temperature of 140 °C. According to the diagrams, the dissolution of copper requires a pH of less than 3.1 and an oxidizing redox potential higher than 0.3 V, but to maintain iron ions in solution and prevent iron precipitation, low pH and the oxidizing redox potential above 0.8 V are required.

## 3 Materials and Procedure

In this research, the chalcopyrite concentration from Sarcheshmeh copper reservoir in Iran was used as a feed for the pressure leaching experiments. The mineralogical composition of the chalcopyrite concentrate was determined by X-ray diffraction (XRD) analysis (Fig. 2). The elemental composition of chalcopyrite concentrate was determined by XRF, as shown in Table 2.

Merck's sulfuric acid was used in leaching experiments. All solutions were made with distilled water. The grain size distribution of copper concentrate is presented in Fig. 3. The results show that the particle size of the chalcopyrite concentrate (d80) was 80% less than 90 μm. The experiments were carried out in a stainless-steel container in an autoclave equipped with a temperature controller, a variable speed stirrer, a barometer, and a heater. 25 g of concentrate sample was added to 250 ml of 2 M sulfuric acid solution in a stainless-steel container with a total volume of 500 ml to reach  $S/L = 0.1$ , and then, the vessel was put into the autoclave. The charged feed was heated under pressure of pure oxygen gas to the required temperature (100–180 °C). When the system reached the required temperature, stirring was started. The stirring rate was maintained at 750 rpm to ensure that the oxygen got dispersed and the reaction was not limited by mass transfer. After the tests, the autoclave was rapidly cooled with water, and the

**Table 1** Reported results of activation energy for chalcopyrite leaching in different media

Medium	Temperature range (°C)	Activation energy (kJ mol <sup>-1</sup> )	References
H <sub>2</sub> So <sub>4</sub> + O <sub>2</sub>	160–180	42.4	[19]
HClO <sub>4</sub> + O <sub>2</sub>	105–120	47.3	[22]
NaNO <sub>2</sub> + H <sub>2</sub> So <sub>4</sub>	80–120	34.06	[23]
H <sub>2</sub> So <sub>4</sub> + NaCl	90–120	15.22	[24]
H <sub>2</sub> So <sub>4</sub> + O <sub>2</sub>	125–140	93.5	[25]
H <sub>2</sub> So <sub>4</sub> + O <sub>2</sub>	80–100	61.93	[26]
H <sub>2</sub> So <sub>4</sub> + H <sub>2</sub> O <sub>2</sub>	30–80	39	[27]
H <sub>2</sub> So <sub>4</sub> + H <sub>2</sub> O <sub>2</sub>	25–50	60	[28]
H <sub>2</sub> So <sub>4</sub> + K <sub>2</sub> Cr <sub>2</sub> O <sub>7</sub>	50–97	24	[29]

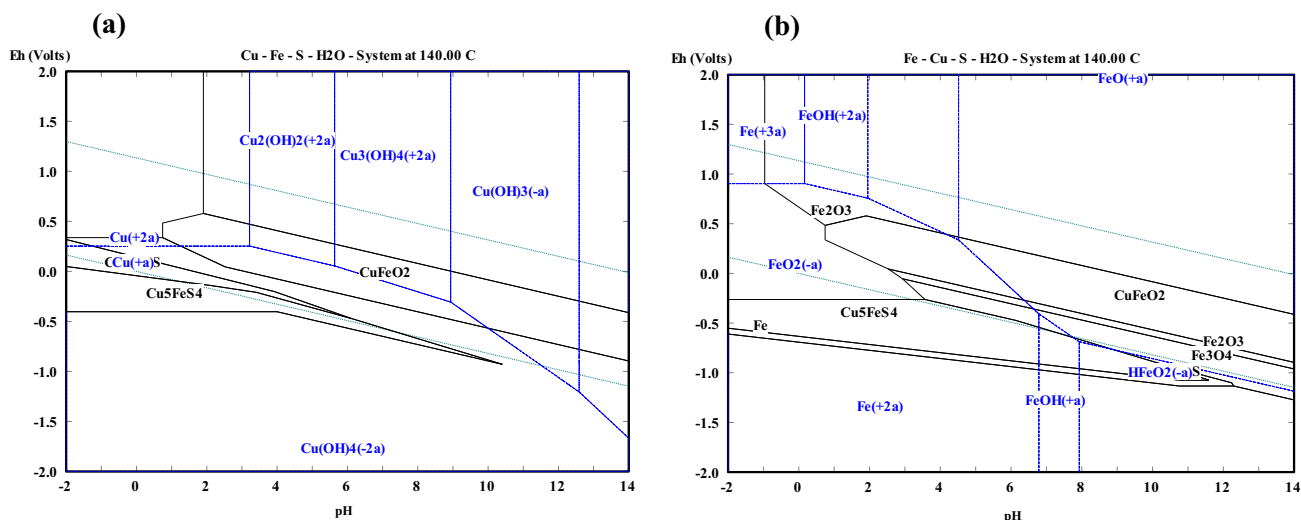


**Fig. 1** Cu–Fe–S Pourbaix diagrams. **a** Based on Cu and **b** based on Fe

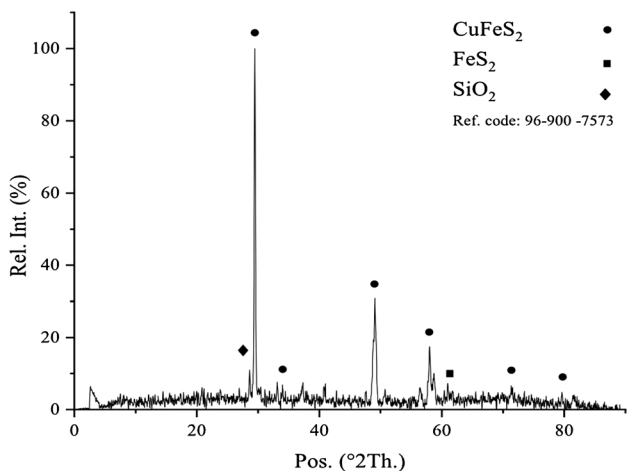


**Fig. 2** XRD pattern of chalcopyrite concentrate

obtained solution was filtered. Concentrations of dissolved copper and iron in the solution were measured using atomic absorption spectrometry (AAS).

X-ray mapping by SEM–EDS for the before leaching sample in Fig. 4 shows how the elements were distributed in the chalcopyrite sample. The specific surface area of the chalcopyrite concentrate was determined to be 0.796  $\frac{m^2}{g}$  by the BET method.

### 4 Design of Experiments

CCD is one of the RSM methods that is the most suitable design for fitting second-order polynomial equations [21]. In this design, the variables are studied at five levels ( $-\alpha, -1, 0, +1, +\alpha$ ). The total number of experiments is as follows:

$$N = 2^k + 2k + n$$

**Table 2** Chemical analysis of the chalcopyrite concentrate

The rest	Si	Mg	Na	S	Fe	Cu	Element
8.22	2.22	1	1.2	36.1	26.7	24.56	Weight percent %

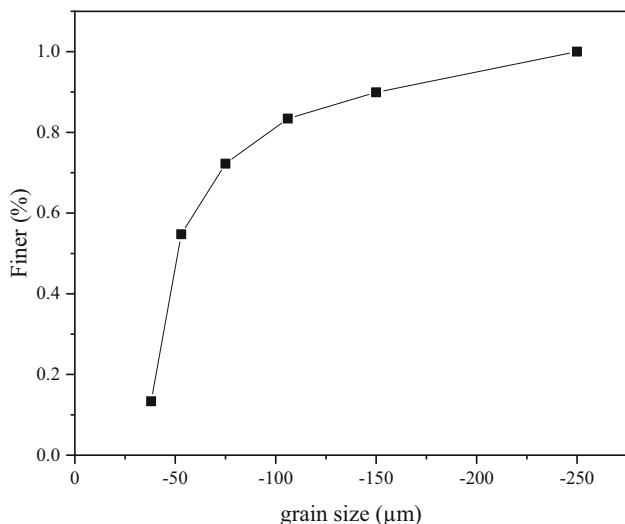


**Fig. 3** Grain size distribution of chalcopyrite sample

where  $N$  is the total number of experiments,  $k$  is the number of factors, and  $n$  is the number of replicates. Central composite design (CCD) was used to investigate the effect of significant factors (oxygen pressure, temperature, and time) and their interactions. These factors were studied at five different levels coded as  $-\alpha$ ,  $-1$ ,  $0$ ,  $+1$ , and  $+\alpha$ , in which the range of oxygen pressure, leaching temperature, and leaching time were from 0.6 to 1 MPa, 100 to 180 °C, and 100 to 240 min, respectively. The primary value and range of variables at levels of  $-1$ ,  $0$ , and  $1$  were determined by trial and error, but the  $\alpha$  levels were determined by the software. The number of  $\alpha$  was 1.681. Dissolution of copper and iron was selected as the system response. The actual and coded values of the factors are summarized in Table 3. Minitab software was employed to design, analyse, and optimize the experiments.

The experimental results of the CCD model are obtained from Eq. 5 [31]:

$$Y = \beta_0 + \sum_{i=1}^k \beta_i X_i + \sum_{i=1}^{k-1} \sum_{j=2}^k \beta_{ij} X_i X_j + \sum_{i=1}^k \beta_{ii} X_i^2 + \varepsilon \quad (5)$$

where  $Y$  is the response variable;  $\beta_0$  is the intercept;  $\beta_i$ ,  $\beta_{ij}$  and  $\beta_{ii}$  are coefficients of the linear effect, double interactions;  $X_i, X_j$  are the independent factors; and  $\varepsilon$  is error.  $Y$  represents the Cu or Fe dissolution.

### 5 Result and Discussion

These 20 tests based on CCD and the response of each test are shown in Table 4. The order of experiments has been arranged randomly.

### 6 Regression and Adequacy of the Model for Copper Dissolution

The results were analyzed by Minitab software. The proposed regression equation for the copper dissolution in uncoded units is as follows:

$$\begin{aligned} \%Cu = & 3.7 + 0.165X_1[^\circ C] - 0.0974X_2[\text{min}] - 24.8X_3[\text{MPa}] \\ & + 0.000150X_1^2 + 0.000235X_2^2 + 12.6X_3^2 \\ & + 0.000758X_1 \times X_2 + 0.1283X_1 \times X_3 - 0.0012X_2 \times X_3 \end{aligned} \quad (6)$$

where  $X_1, X_2$ , and  $X_3$  are temperature, time, and pressure, respectively. The significance of each factor in the model was determined using  $F$ -value and  $p$ -value. If the  $F$ -value is higher than the critical value and the  $p$ -value is less than 0.05, it shows that the model is well-fitted to experimental data. The results of variance analysis are summarized in Table 4. The 95% confidence level ( $\alpha = 0.05$ ) was used to determine statistical significance. As shown in Table 5, the  $p$ -value less than 0.05 indicates that the model is significant, and there will be an acceptable performance in the prediction of response. The terms with  $p$ -values more than 0.05 are insignificant, and they can be omitted from the model. Hence, they were removed from the model. The obtained final equation for copper dissolution with significant terms is as follows:

$$\begin{aligned} \%Cu = & -27.01 + 0.3101X_1 - 0.0184X_2 + 13.06X_3 \\ & + 0.000758X_1 \times X_2 \end{aligned} \quad (7)$$

The coefficient of regression ( $R^2$ ) for fitness of the model and adjusted  $R^2$  for confirmation of the model adequacy were used to evaluate the proposed model in terms of its proximity to the actual system. The obtained equation, in terms of actual factors, can predict the percentage of copper dissolution according to the given values of the specified range for each factor. Removing the nonsignificant terms of the model causes a change in the  $R^2$  values of the model. Table 5 shows their values before and after removing these terms. According to Table 6, although

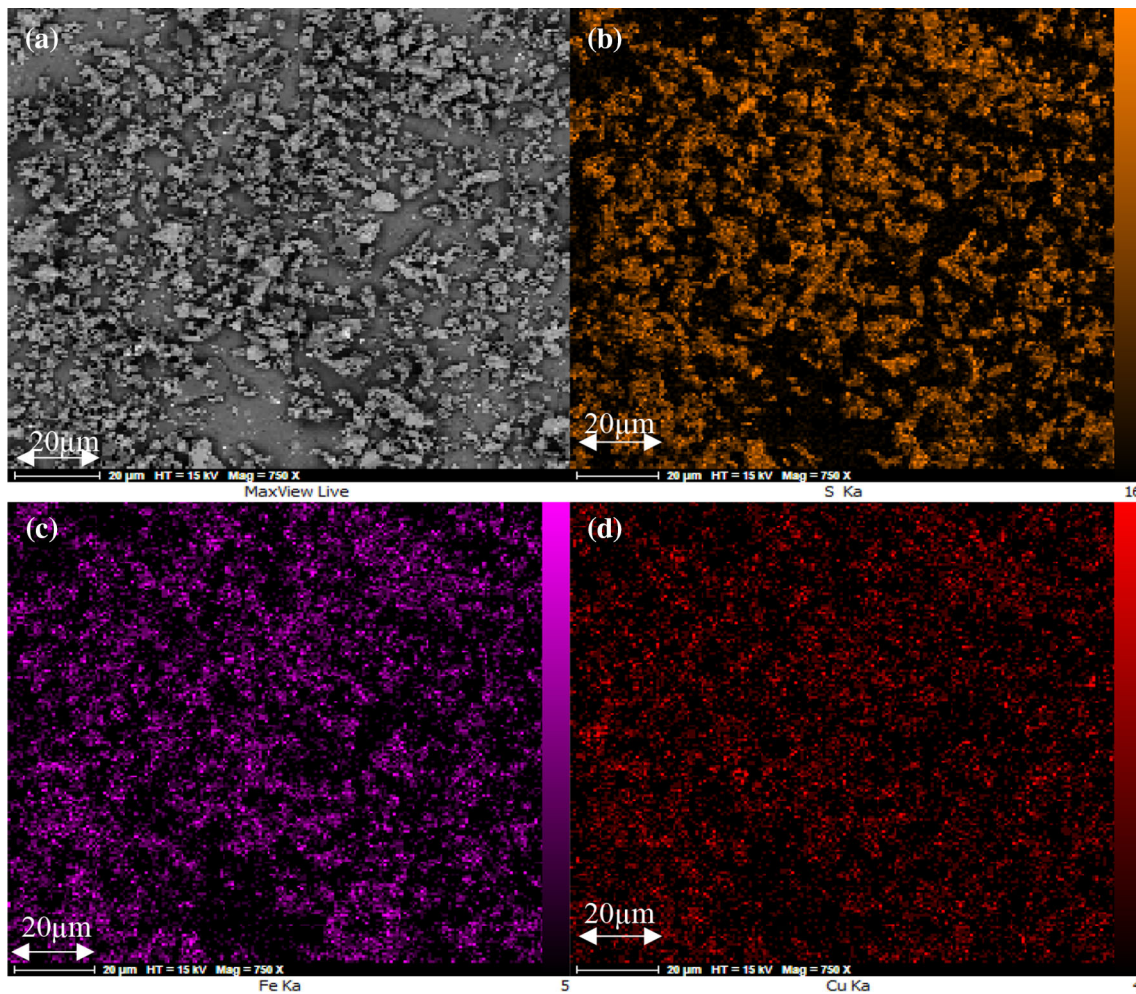


**Fig. 4** X-ray mapping by SEM-EDS of unleached chalcopyrite particles. **a** BSE Image **b** S **c** Fe **d** Cu

**Table 3** Central composite design (CCD) using response surface methodology (RSM), range, and levels of variables

Variables	Levels				
	$-\alpha$	$-1$	$0$	$+1$	$+\alpha$
Temperature (C°)	72.728	100	140	180	207.272
Time (min)	52.275	100	170	240	287.725
Oxygen pressure (MPa)	0.46	0.6	0.8	1	1.136

the  $R$ -square decreases slightly, the increase in  $\text{pred-}R^2$  makes the model more accurate than the previous one.

The normal probability plot shows the status of residuals relative to a straight line. If residuals follow this line, it indicates that they have a normal distribution. According to Fig. 5, the residuals follow a straight line illustrating the normal distribution of errors. The model’s  $P$ -value less than 0.05 and the Lack-of-Fit’s  $P$ -value more than 0.05 imply that the model is significant.

### 7 Regression and Adequacy of the Model for Iron Dissolution

The final equation obtained for iron dissolution by software with significant terms is as follows:

$$\begin{aligned} \%Fe = & -70.2 + 1.028X_1[^\circ C] - 0.1135X_2[\text{min}] + 12.88X_3[\text{MPa}] \\ & - 0.002971X_1^2 + 0.001594X_1 \times X_2 \end{aligned} \tag{8}$$

**Table 4** Actual level of independent variables along with the observed values for the response variable

Std	Run	Factor 1 A: temperature (°C)	Factor 2 B: time (min)	Factor 3 C: pressure (MPa)	Response 1 Cu (%)	Response 2 Fe (%)
9	1	72.7283	170	0.8	11.6667	6.112
8	2	180	240	1	73.109	72.658
18	3	140	170	0.8	43.0692	48.631
6	4	180	100	1	57.1069	48.8462
15	5	140	170	0.8	42.333	46.594
17	6	140	170	0.8	39.016	45.7692
20	7	140	170	0.8	39.6627	44.598
3	8	100	240	0.6	26.73	16.887
1	9	100	100	0.6	19.17	12.4231
11	10	140	52.27	0.8	30.91	32.3654
7	11	100	240	1	30.0368	24.0769
12	12	140	287.7	0.8	47.6667	58.7692
16	13	140	170	0.8	38.1973	43.165
4	14	180	240	0.6	63.95	67.165
10	15	207.2	170	0.8	68.875	61.5385
19	16	140	170	0.8	40.875	44.369
14	17	140	170	1.13	44.1667	48.975
5	18	100	100	1	24.7604	16.1897
13	19	140	170	0.46	37.8583	41.36
2	20	180	100	0.6	49.625	42.9231

**Table 5** Analysis of variance (ANOVA) of the response surface for copper extraction

Source	DF	Adj SS	Adj MS	F-value	P-value
Model	9	4885.00	542.78	121.21	0.000
Linear	3	4819.06	1606.35	358.72	0.000
$X_1$	1	4211.22	4211.22	940.43	0.000
$X_2$	1	514.64	514.64	114.93	0.000
$X_3$	1	93.20	93.20	20.81	0.001
Square	3	21.47	7.16	1.60	0.251
$X_1^2$	1	0.84	0.84	0.19	0.675
$X_2^2$	1	19.15	19.15	4.28	0.066
$X_3^2$	1	3.65	3.65	0.81	0.388
2-Way Interaction	3	44.48	14.83	3.31	0.066
$X_1 \times X_2$	1	36.04	36.04	8.05	0.018
$X_1 \times X_3$	1	8.43	8.43	1.88	0.200
$X_2 \times X_3$	1	0.00	0.00	0.00	0.982
Error	10	44.78	4.48		
Lack-of-Fit	5	26.48	5.30	1.45	0.348
Pure Error	5	18.30	3.66		
Total	19	4929.78			

where  $X_1$ ,  $X_2$ , and  $X_3$  are similar to the preceding equation. The summary of statistical analysis (Table 7) and adequacy of the model were justified by the analysis of variance (Table 8).

Based on Table 7, the  $R^2$  value of 0.9793 depicts the high fitness of the model. The high value of the adjusted  $R^2$  (0.9719) and the prediction  $R^2$  (0.9311) further prove the adequacy of the model. The normal probability of residuals

**Table 6** R-square values before and after removing nonsignificant terms of the model

	Full quadratic model	Modified model
$R^2$	0.9909	0.9849
Adj- $R^2$	0.9827	0.9808
Pred- $R^2$	0.9535	0.9711

is shown in Fig. 6, which represents the normal and independent distribution of errors.

### 8 Response Surface Analysis

Minitab software was used to develop 3D response surface plot. The 3D plots are graphical representation of the influence of parameters on the response surface and one of the useful ways to reveal optimal response conditions. The effect of variables on the response (%Cu and Fe) is shown in Fig. 7. In these plots, the effect of two factors on the response surface is presented, while the other one is fixed at the center point level. Figure 7a, b shows the interaction effect of temperature–time and temperature–oxygen pressure on the %Cu, indicating that temperature is the most important factor in the copper dissolution. Increasing time and pressure also have a positive effect on the response. The interaction between time and pressure is shown in Fig. 7c, indicating that the influence of these two variables on the response surface is alike. The interaction between temperature–time and temperature–pressure on iron dissolution are shown in Fig. 7c, e, respectively. Unlike copper, increasing temperature during the short leaching time first

**Table 7** Summary of statistical analysis for iron extraction

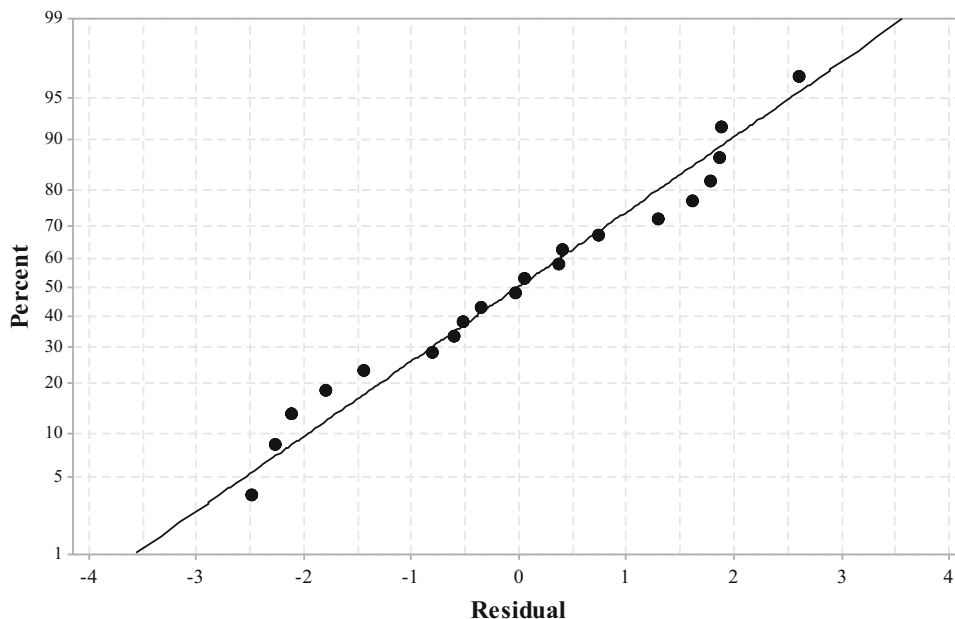
S	R-sq	R-sq(adj)	R-sq(pred)
2.11612	97.93%	97.19%	93.11%

increases %Fe and then decreases. Figure 7f illustrates the effect of the interaction between pressure and time on iron dissolution. By comparing Fig. 7a, d, in a short time and high temperatures, copper dissolution is more than iron. Also, Fig. 7b, e represents the same effect of oxygen pressure on copper and iron extraction. Minitab software was used to determine optimum conditions. The optimum conditions are defined with the aim of maximum copper dissolution. Optimal conditions were determined at  $t = 287.7$  min,  $P = 1.13$  MPa, and  $T = 207$  °C. Under these conditions, 93.08% of copper was extracted. The optimal conditions with the predicted and experimental percentages of copper and iron dissolution are shown in Table 9.

To recover remaining copper of leached chalcopyrite, methods exerted for low-grade concentrates such as heap leaching or heap bioleaching [32, 33] can be used. Iron is considered an impurity in PLS solution, but it can be removed from PLS by precipitation and SX process.

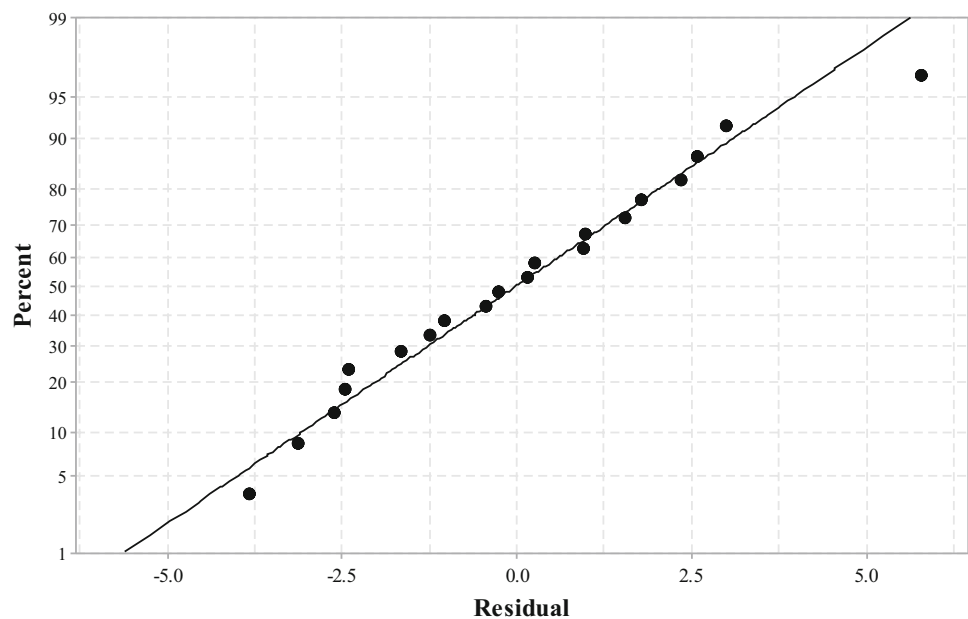
First, it may seem that the high agitation rate causes the passive layer to be separated from the surface of the spherical particles. But since the temperature of experiments is higher than the melting point of elemental sulfur ( $T > 115$  °C), they cause this element to be melted on the surface of particles. Hence, the diffusion process will be hindered from this melted layer. Figure 8 shows X-ray

**Fig. 5** Normal probability plot of residuals for %Cu responses



**Table 8** Analysis of variance (ANOVA) of the response surface quadratic model for iron extraction

Source	DF	Adj SS	Adj MS	F-value	P-value
Model	9	6174.83	686.09	61.81	0.000
Linear	3	5665.01	1888.34	170.11	0.000
Temperature	1	4770.00	4770.00	429.71	0.000
Time	1	804.38	804.38	72.46	0.000
Pressure	1	90.62	90.62	8.16	0.017
Square	3	349.34	116.45	10.49	0.002
Temperature*temperature	1	346.21	346.21	31.19	0.000
Time*time	1	8.10	8.10	0.73	0.413
Pressure*pressure	1	11.45	11.45	1.03	0.334
Two-way interaction	3	160.48	53.49	4.82	0.025
Temperature*time	1	159.34	159.34	14.35	0.004
Temperature*pressure	1	0.03	0.03	0.00	0.962
Time*pressure	1	1.12	1.12	0.10	0.757
Error	10	111.01	11.10		
Lack-of-fit	5	92.39	18.48	4.96	0.052
Pure error	5	18.61	3.72		
Total	19	6285.84			

**Fig. 6** Normal probability plot of residuals for %Fe responses

mapping of leached residue under conditions of  $T = 180\text{ }^{\circ}\text{C}$ ,  $t = 4\text{ h}$ , and  $P = 1\text{ MPa}$  (Test # 2). As shown in Fig. 9, it can be seen that the elemental sulfur is formed and it adheres to the chalcopyrite particles. Although the temperature and pressure are at high levels, the formation of elemental sulfur prevents the dissolution process. The leaching residue, which was obtained under the above conditions, was characterized by XRD (Fig. 10). According to the XRD spectrum,  $\alpha$ -sulfur is produced during chalcopyrite leaching. The BET surface area of the reacted

sample is determined to be  $0.55\frac{\text{m}^2}{\text{g}}$ . Based on the obtained results, the primary leaching equation is accomplished according to Eq (1).

## 9 Kinetics Study of the Process

Several research works have been carried out on the kinetics and mechanism of chalcopyrite leaching in different media with various oxidants. In the present work, the



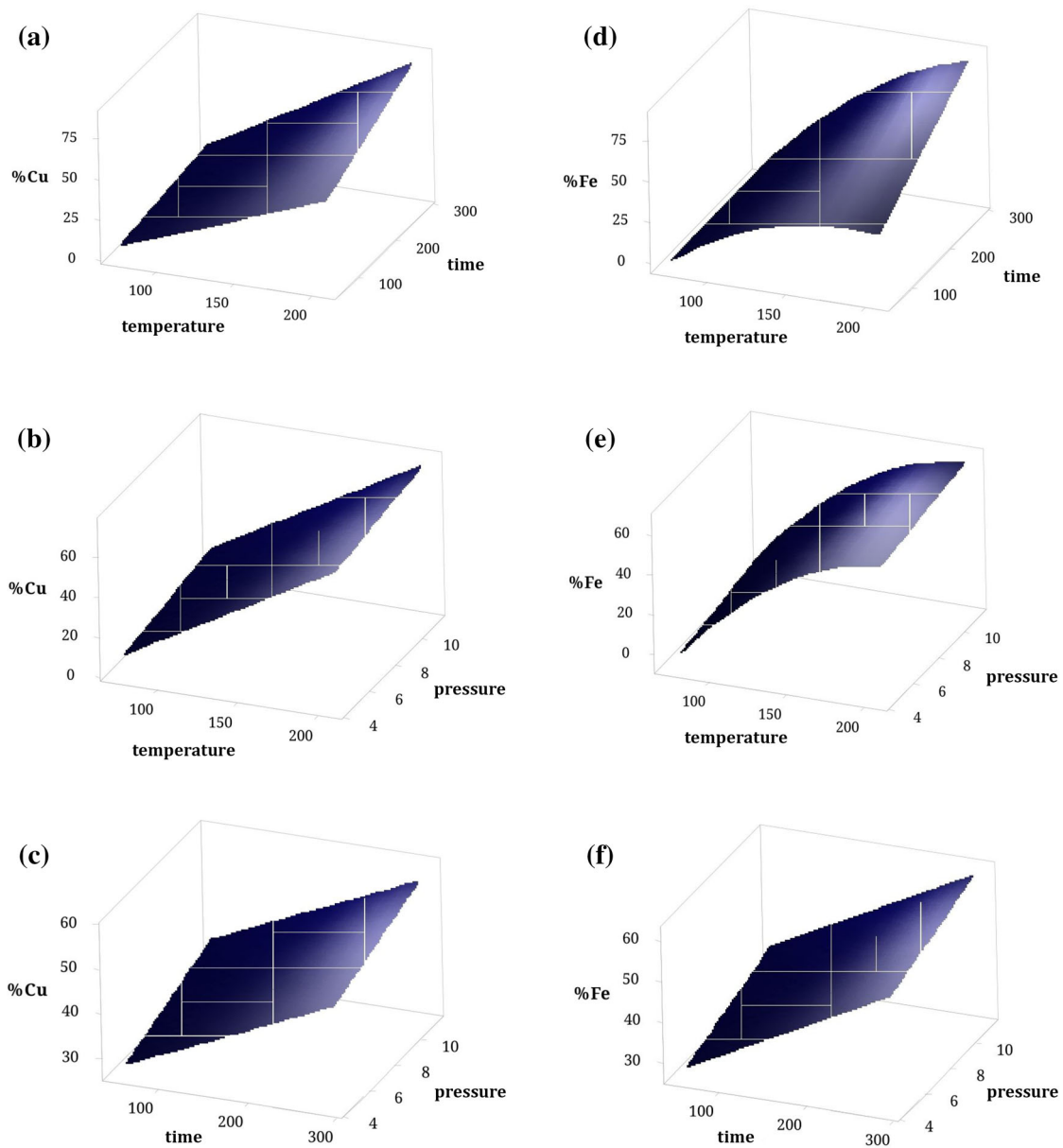


**Fig. 7** Surface plot for the interaction of variables on the copper and iron extraction

**Table 9** Optimal conditions for proper leaching of chalcopyrite concentrate

Optimal conditions			Percentage of metals dissolution			
Temperature (°C)	Time (min)	Pressure (MPa)	Predicted Cu	Experimental Cu	Predicted Fe	Experimental Fe
207.27	287.72	1.136	%94.23	%93.08	%94.4	%92.2

kinetics and mechanism of pressure leaching of chalcopyrite were investigated. A shrinking core model (SCM) was used to determine the leaching process kinetics. In this model, it is assumed that the reaction first begins from the external shell of the spherical solid particle, and then, the

reaction zone (ash) moves toward the inner surface of the solid core. According to the model, it can be considered that the leaching process consists of three major steps. The slowest step controls the process kinetics: (1) mass transfer from the fluid layer around the solid core, (2) chemical

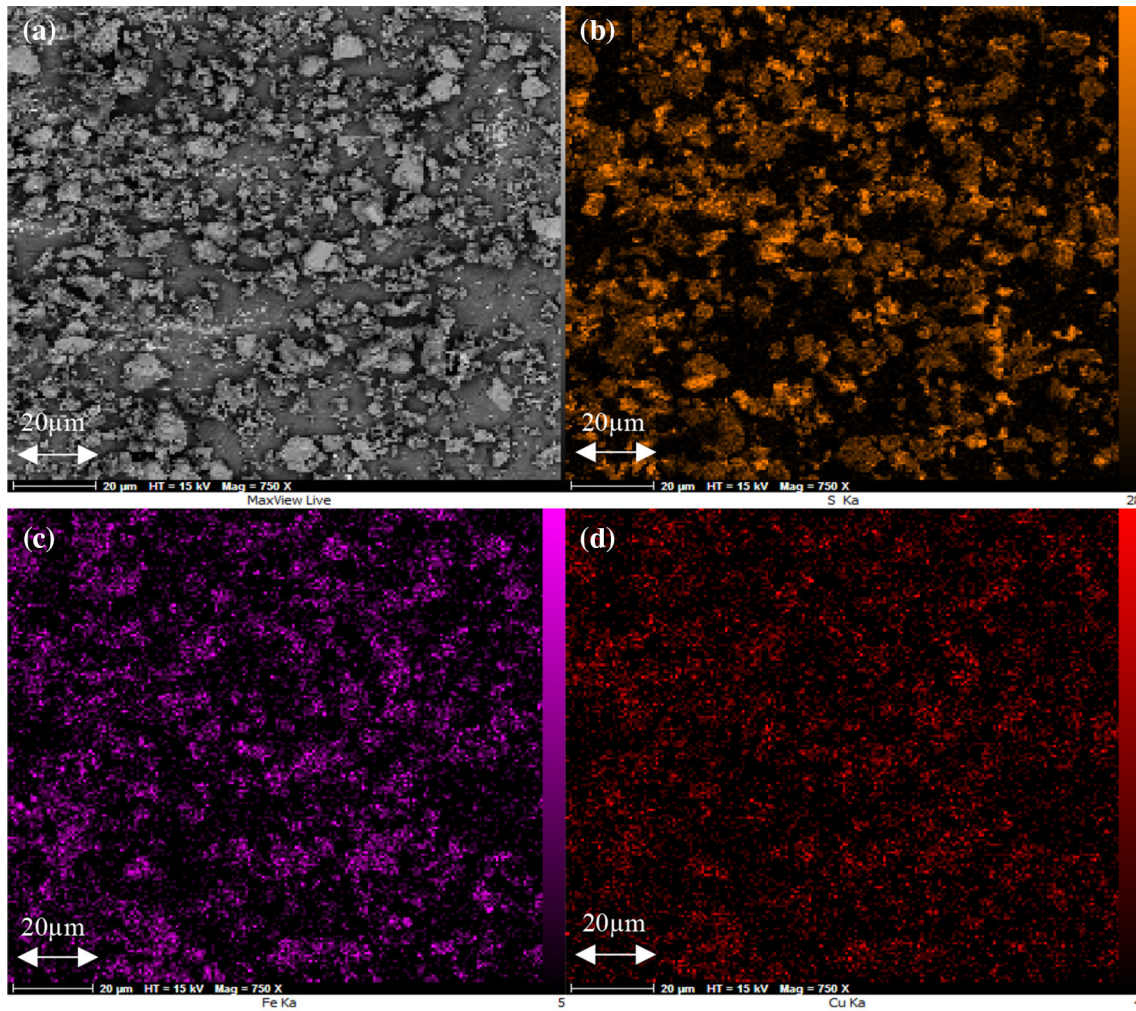


**Fig. 8** SEM–EDS mapping of leached chalcopyrite particles. **a** BSE image, **b** S, **c** Fe, and **d** Cu

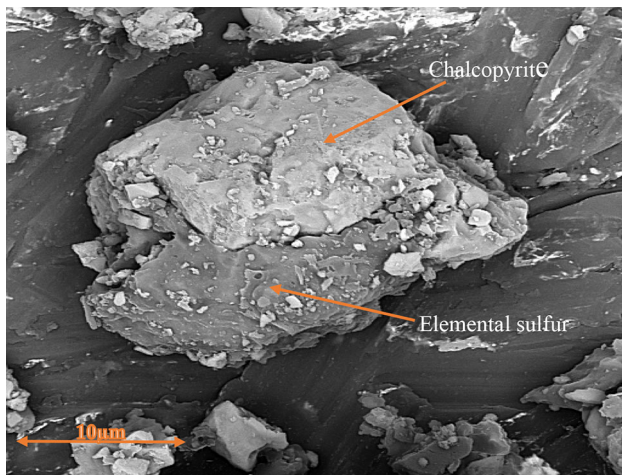


**Fig. 9** FESEM-BSE image of leached chalcopyrite particle (oxygen pressure: 1 MPa, temperature: 180 °C, and leaching time: 4 h)

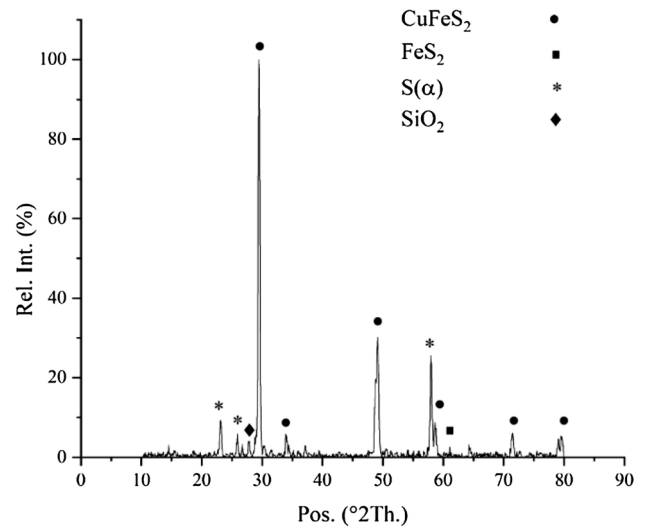


**Fig. 10** XRD pattern of solid residue

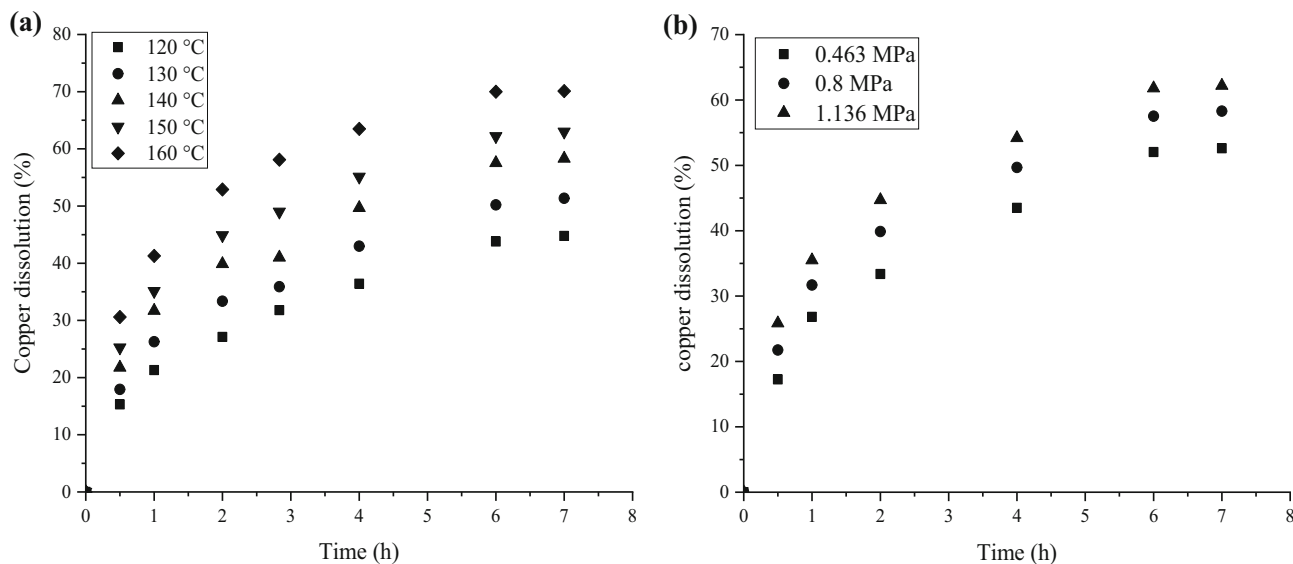


**Fig. 11** Effects of variables on the rate of copper leaching. **a** Temperature effect and **b** oxygen pressure effect. (H2SO4 concentration: 2.0 M, agitation speed: 750 rpm, and S/L = 0.1)

**Table 10** Results for the kinetic constants and correlation coefficients for shrinking core model at different temperatures and oxygen pressures

Models		Temperature (°C)					Oxygen pressure (MPa)		
		120	130	140	150	160	0.46	0.8	1.13
$\alpha = k_f t$	$R^2$	0.6169	0.5855	0.5255	0.4981	0.45	0.6055	0.5258	0.4525
	$k_f$	0.24	0.251	0.259	0.279	0.2795	0.247	0.259	0.2683
$1 - (1 - \alpha)^{\frac{1}{3}} = k_r t$	$R^2$	0.8656	0.8555	0.8262	0.8282	0.8266	0.859	0.8262	0.796
	$k_r$	0.1179	0.1263	0.1329	0.141	0.154	0.123	0.1329	0.1411
$1 - \frac{2}{3}\alpha - (1 - \alpha)^{\frac{2}{3}} = k_d t$	$R^2$	0.9961	0.9989	0.9965	0.9966	0.9942	0.9971	0.9965	0.9912
	$k_d$	0.0321	0.0358	0.0388	0.0425	0.0487	0.0343	0.0388	0.0425

reaction on the solid and liquid interface, and (3) diffusion through the ash layer. The equations for these steps are:

$$\alpha = k_f t \tag{9}$$

$$1 - (1 - \alpha)^{\frac{1}{3}} = k_r t \tag{10}$$

$$1 - \frac{2}{3}\alpha - (1 - \alpha)^{\frac{2}{3}} = k_d t \tag{11}$$

where  $k_f$ ,  $k_r$ , and  $k_d$  are kinetic constants,  $\alpha$  is the fraction reacted, and  $t$  is the reaction time. To determine the mechanism of the process, the effect of temperature and oxygen pressure variables on the leaching process was investigated. Figure 11a, b shows the effect of temperature and pressure on copper dissolution, respectively. During the study of temperature effect, the pressure was maintained at 0.8 MPa (center point level), and during the study of pressure effect, the temperature was maintained at 140 °C.

After the tests, the correlation of different kinetics models was examined (the three above mentioned models) with the obtained data. The kinetic equations with their linear correlation coefficients and kinetic constant are presented in Table 10.

As can be seen in Table 9, model 3 is in close agreement with the data. It can be due to the formation of the elemental sulfur layer produced by reaction 1. Arrhenius equation shows the kinetic dependence of the dissolution process on temperature [34] that is shown as follows:

$$k = A_0 \exp\left(\frac{-E}{RT}\right)$$

where  $k$  is the kinetic constant,  $A_0$ ,  $E_a$ ,  $R$ , and  $T$  are pre-exponential factor, activation energy, the universal gas constant, and absolute temperature, respectively. By drawing the  $\ln k$  versus  $\frac{1000}{T}$ , the obtained line slope shows  $\frac{-E_a}{R}$ . It is represented in Fig. 12.

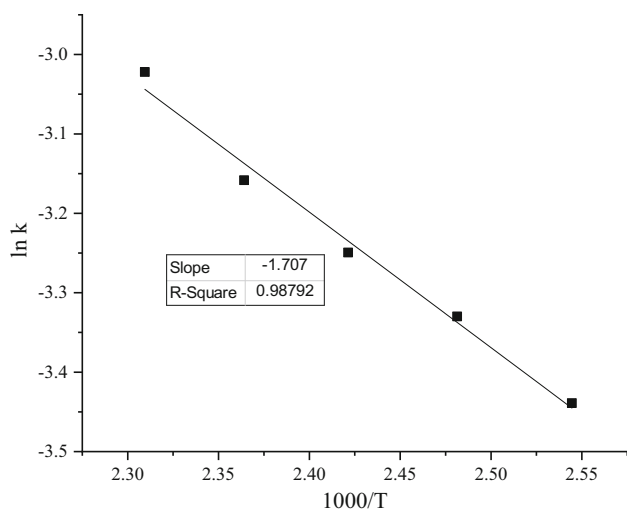


**Fig. 12** Arrhenius plot for chalcopyrite concentrate dissolution by pressure leaching

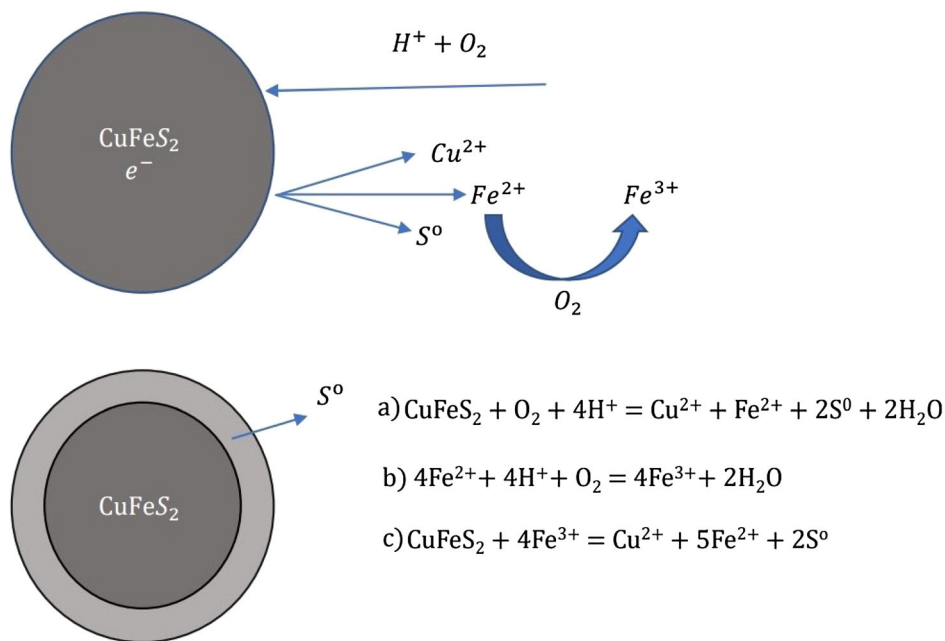
The activation energy obtained is 14.19 kJ.mol, which is less than 40 kJ/mol. It indicates that the diffusion mechanism from the produced layer controls the process. The formation of elemental sulfur illustrates that the main leaching equation is accomplished as shown in Fig. 13a. In addition, the presence of oxygen in the acidic solution causes conversion of  $Fe^{2+}$  to  $Fe^{3+}$  (Fig. 13b). It can contribute in the leaching process matching to Fig. 13c.

### 10 Conclusion

In this research, the pressure leaching of chalcopyrite concentrate was investigated in sulfuric acid solution. The experiments were designed by CCD to optimize the variables with the goal of maximum copper dissolution. The results are as follows.

1. Temperature is the most important factor in the dissolution of copper, and increasing oxygen pressure has a positive effect of chalcopyrite leaching
2. Under the optimal conditions, the maximum copper dissolution reaches 93.08%.
3. Unexpectedly, according to FESEM-BSE image, the elemental sulfur is formed at high temperature ( $T = 180\text{ }^{\circ}\text{C}$ ) and hinder the leaching process which can be due to the high percentage of sulfur in the chalcopyrite sample.
4. A linear model for %Cu and a quadratic model for %Fe have been proposed by Minitab software. Both models are well-fitted to experimental data that can be confirmed by the high  $R^2$ , adj- $R^2$ , and pred- $R^2$  values.
5. The kinetics studies of the process shows that the diffusion of the produced layer control the dissolution process and the activation energy obtained is 14.19 kJ/mol.

**Fig. 13** Mechanism of chalcopyrite leaching



## References

1. Davenport W G, King M J, Schlesinger M E, and Biswas A K, *Extractive Metallurgy of Copper*, (4th ed), Pergamon (2002).
2. Baba A A, Ayinla K I, Adekola F A, Ghosh M K, Ayanda O S, Bale R B, Sheik A R, and Pradhan S R, *Int J Min Eng Miner Process*, **1** (2012) 1.
3. Li Y, Kawashima N, Li J, Chandra A, and Gerson A A, *Adv Colloid Interface Sci*, **197** (2013) 1.
4. Pradhan N, Nathsarma K C, Srinivasa Rao K, Sukla L B, Mishra B K, *Miner Eng*, **21** (2008) 355.
5. Koleini S M J, Aghazadeh V, and Sandström A, *Miner Eng*, **24** (2011) 381.
6. Chiluiza E L R, and Donoso P N, *J Mex Chem Soc* **60** (2016) 238.
7. Guan Y C, and Han K N, *Metall Mater Trans B* **28** (1997) 979.
8. Hernández P C, Taboada M E, Herreros O O, Graber T A, and Ghorbani Y, *Minerals* **8** (2018) 238.
9. Hiroyoshi N, and Kuroiwa S, *Hydrometallurgy* **74** (2004) 103.
10. Dutrizac J E, *Can Metall Q* **28** (1989) 337.
11. Pinches A, Al-Jaid F O, Williams D J A, *Hydrometallurgy* **2** (1976) 87.
12. Turan M D, and Altundoğan H S, *Metall Mater Trans B* **44** (2013) 809.
13. McDonald R G, and Muir D M, *Hydrometallurgy* **86** (2007) 191.
14. Hackl R P, Dreisinger D B, Peters E, King J A, *Hydrometallurgy* **39** (1995) 25.
15. Hiroyoshi N, Arai M, Miki H, Tsunekawa M, Hirajima T, *Hydrometallurgy* **63** (2002) 257.
16. Holliday R I, and Richmond W R, *J Electroanal Chem Interfacial Electrochem* **288** (1990) 83.
17. Yu P H, Hansen C K, and Wadsworth M E, *Metall Trans* **4** (1973), 2137.
18. Vizsolyi H V, Warren I H, and Mackiw V N, *Metals* **19** (1967) 52.
19. Han B, Altansukh B, Haga K, Takasaki Y, and Shibayama A, *J Sustain Metall* **3** (2017) 528.
20. Montgomery D C, *Design and Analysis of Experiments Response Surface Method and Designs*, Wiley, New Jersey (2005).
21. Bezerra M A, Santelli R E, Oliveira E P, Villar L S, and Escalera L A, *Talanta* **76** (2008) 965.
22. Peters E, and Loewen F, *Metall Trans* **4** (1973) 5.
23. Gok O, Anderson C G, Cicekli G, and Cocen E L, *Physicochem Prob Min Process* **50** (2014).
24. Qiu T S, Nie G H, Wang J F, and Cui L F, *Trans Nonferr Metals Soc China* **17** (2007) 418.
25. Padilla R, Pavez P, and Ruiz M C, *Hydrometallurgy* **91** (2008) 113.
26. Cháidez J, Parga J, Valenzuela J, Carrillo R, and Almaguer I, *Metals* **9** (2019) 189.
27. Adebayo AO, Ipinmoroti KO, Ajayi OO, *Chem Biochem Eng Q* **17** (2003) 213.
28. Antonijević M M, Janković Z D, and Dimitrijević M D, *Hydrometallurgy* **71** (2004) 329.
29. Aydogan S, Ucar G, and Canbazoglu M, *Hydrometallurgy* **81** (2006) 45.
30. Garverick L, (ed) *Corrosion in the petrochemical industry*, ASM international (1994) p 77.
31. Turan M D, Arslanoğlu H, and Altundoğan H S, *J Taiwan Inst Chem Eng* (2015).
32. McBride D, Gebhardt J, Croft N, and Cross M, *Minerals* **8** (2018) 9.
33. Panda S, Sanjay K, Sukla L B, Pradhan N, Subbaiah T, Mishra B K, Prasad M S R, and Ray S K, *Hydrometallurgy* **125** (2012) 157.
34. Han B, Altansukh B, Haga K, Takasaki Y, and Shibayama A, *Leaching and Kinetic Study on Pressure Oxidation of Chalcopyrite in H<sub>2</sub>SO<sub>4</sub> Solution and the Effect of Pyrite on Chalcopyrite Leaching*, The Minerals, Metals & Materials Society (2017).

**Publisher's Note** Springer Nature remains neutral with regard to jurisdictional claims in published maps and institutional affiliations.